KFKI-1988-33/C

K. SZEGŐ
I. TÓTH
Z. SZATMÁRY
B.A. SMITH
A. KONDOR
E. MERÉNYI

DUST PHOTOMETRY IN THE NEAR NUCLEUS REGION OF COMET HALLEY

Hungarian Academy of Sciences

CENTRAL
RESEARCH
INSTITUTE FOR
PHYSICS

BUDAPEST

KFKI-1988-33/C
PREPRINT

DUST PHOTOMETRY IN THE NEAR NUCLEUS REGION OF COMET HALLEY

K. SZEGÖ, I. TÓTH*, Z. SZATMÁRY, B.A. SMITH**,
A. KONDOR, E. MERÉNYI

Central Research Institute for Physics
H-1525 Budapest 114, P.O.B. 49, Hungary

*Konkoly Observatory, H-1121 Budapest,
Konkoly Thege M. 13-17, Hungary

**Lunar and Planetary Laboratory, University of Arizona,
Tucson, AZ 85721, USA

HU ISSN 0368 5330

K. Szegő, I. Tóth, Z. Szatmáry, B.A. Smith, A. Kondor, E. Merényi: Dust photometry in the near nucleus region of comet Halley. KFKI-1988-33/C

ABSTRACT

The dust-jet radial brightness has been analysed along jet cores on images taken by the TV experiment aboard VEGA-2 spacecraft on 9 March 1986 during the close encounter with Comet Halley. Applying the RFIT code - used in reactor physics - to the data, it has been shown that there is a break-point in the radial brightness distribution which occurs at about 40 km above the surface.

We interpret this result as being due to heat-shock included desintegration of dust particles as they are ejected into the near-nucleus environment.

К. Серё, И. Тот, З. Сатмари, Б.А. Смит, А. Кондор, Э. Мерени: Пылевая фотометрия в окрестности ядра кометы Галлея. KFKI-1988-33/C

АННОТАЦИЯ

На фотографиях, полученных с помощью бортовой телевизионной системы КА "Вега-2" 9 марта 1986 г. во время наибольшего сближения с кометой Галлея, изучались изменения яркости пылевых джетов (выбросов) в радиальном направлении. Применив первоначально предназначенный для реакторно-физических расчетов пакет программ RFIT, на расстоянии 40 км от поверхности кометы удалось обнаружить точку излома в распределении яркости. Этот результат интерпретируется как доказательство того, что выбрасывающиеся с поверхности в окрестности ядра кометы пылевые частицы распыляются под действием теплового шока.

Szegő K., Tóth I., Szatmáry Z., B.A. Smith, Kondor A., Merényi E.: Por-fotometria a Halley üstökös magjának közelében. KFKI-1988-33/C

KIVONAT

A por jetek radiális irányu fényességváltozását vizsgáltuk azokon a képeken, amelyeket a Vega-2 ürszonda fedélzeti TV készüléke 1986. március 9-én, a Halley üstökössel való találkozásakor készitett. Az RFIT programcsomag alkalmazásával - amelyet reaktorfizikai számitásokra dolgoztak ki - kimutattuk, hogy a fényességeloszlásokban töréspont van, a felszintől kb. 40 km távolságban.

Ezt az eredményt annak bizonyitékának tartjuk, hogy a felületet elhagyó porszemcsék az elszenvedett hősokk hatására porlódnak az üstökös közeli környezetében.

Abstract

The dust-jet radial brightness has been analysed along jet cores on images taken by the TV experiment aboard VEGA-2 spacecraft on 9 March 1986 during the close encounter with Comet Halley. Applying the RFIT code - used in reactor physics - to the data, it has been shown that there is a breakpoint in the radial brightness distribution which occurs at about 40 km above the surface.

We interpret this result as being due to heat-shock included desintegration of dust particles as they are ejected into the near-nucleus environment.

1. Introduction

Cometary activity manifests itself in dust and gas emission, resulting in coma, jets and tail phenomena. Many of these can be analysed from the ground, but the near-nucleus structure of the emission can only be resolved by close encounters. We summarize here those results of dust photometry which were obtained by analysis of the Comet Halley near nucleus imaging data set obtained by the TV experiment on the VEGA-2 spacecraft on 9 March 1986.

Intuitively, it is easy to distinguish between coma and jets, both of which are mixtures of dust and gas. The coma represents the spatially unstructured surroundings of the nucleus varying only slowly in time; jets, on the other hand, exhibit both structure and rapid time variability. Jets can always be associated with a discrete source region. Visually, however, the brightness difference is rarely sufficient enough to distinguish jets against the coma background. Although the dust-to-gas ratio is more or less constant in the coma, it tends to vary in jets. We already have evidence of pure gas jets in Comet Halley [Cosmovici et al. 1988], but the dust component of the Halley dust jets remains an open question; it may be the same as in the coma or very much different. Observational evidence is lacking.

In the remote images taken by the VEGA-1 and 2 spacecraft the coma dominated the images, showing the same shape around the nucleus as was seen from ground observations. Image enhancement was required to reveal the jet structure [Abergel et al., 1987]. So, it was somewhat of a surprise that in the near encounter images the extended coma was completely missing. The reason, of course, is that the near encounter images were exposed to record the nucleus and the jets, both of which have higher surface brightness than the coma. Nearly all activity was concentrated around the sunlit hemishpere and much of it was structured into discrete jets. This observation has already strongly influenced the modeling of cometary activity, and we shall not discuss it further here. We note only that the near nucleus imaging data are particularly well suited to analyze jets.

As the first step, the position of the jet sources were identified [Smith et al., 1986] both on spherical coordinates centered on the nucleus and on the nucleus itself. The most prominent fans and jets were emitted from a well-defined, narrow, linear feature on the surface, consisting of smaller linear and pointlike sources. This large feature crossed local noon and extended some 70 degrees southward and about 40 degrees to north (directions are defined according to the ecliptic coordinate system). This same analysis also provided the spatial orientation of the jet features. Hence, in what follows, all distances along jets denote true, as opposed to projected, distances from the surface of the nucleus. The emitted dust fan formed an extended, structured, thin dust sheet which was crossed by the spacescraft; one of the images was actually taken within the sheet. The optical density of the dust was also estimated [Sagdeev et al., 1985] and it was concluded that the dust between the spacecraft and the surface is optically thin. It is, however, more difficult to estimate the actual optical density of the jet features.

The common wisdom is that jet formation follows the Finston-Probstein type interaction of the dusty gas emitted by the sun-irradiated surface, i.e. that the emitted gas accelerates the dust, with lighter particles reaching the gas velocity and the heavier laging behind. The dust component is sufficiently tenuous that dust-dust interaction is negligible. In numerical calculations it has always been assumed that dust does not disintegrate into smaller pieces. Although models differ in complexity, they more or less agree that dust particles reach terminal velocity about 10 km from the surface where dust and gas decouple, the most significant part of the acceleration takes place within 1-2 km from the surface [see e.g. Gombosi et al., 1982]. The terminal velocity of a 1 micron size particle is about 0.5-0.7 km/s. The envelope of the jets was estimated in [Sagdeev et al. 1987], with the opening angle of the cone increasing as $r^{1/3}$.

A more refined analysis was performed by Kitamura [1986], who noted that dust in jets should tend to concentrate close to the jet boundary. Observational evidence, however, does not support this. In a more advanced version of his model [Kitamura, 1987] this effect disappeared. Contrary to expectations, many small size dust particles were registered during the VEGA and GIOTTO missions [Grün et al., 1987].

2. Data description

The data set employed in this analysis consists of 11 512x512 pixel size VEGA-2 imaging frames taken over a 15-minute interval starting approximately 370 s before closest approach to the nucleus and continuing 560 s afterwards. The distance to the nucleus was always less than 45 000 km and became as close as 8030 km. The pertinent data for each of these images are summarized in Table 1, together with the bandwidth of the filters used. The images have been photometrically corrected, and quasi-coherent high frequency noise was removed by Fourier filtering.

The images were further processed by median filtering to diminish spike noise. Median filters have proven to be especially effective for this purpose and, although it is a nonlinear transformation, the results presented by Justusson [1981] convince us that the photometric integrity is well preserved.

On the images described above, 10 or 11 distinct jet features can be identified. We have selected 4 well-defined features for further analysis, 3 jet cores and a region which is outside identifiable jet boundaries.

We identify the features in the same way as in [Smith et al., 1986], with a sphere centered on the nucleus, where local noon at the time of encounter defines the zero meridian and the equator plane. Within this system the jets A, B and C were oriented to b= -67°, -54° and -40°, respectively (b is the ecliptic latitude); and all were close (within 5°) to the zero meridian line. The feature D is a radial region outside the identifiable jet features between jets A and B on the images; it has no specific orientation in space.

Because the nucleus is overexposed on most of our images [Sagdeev and Szego, 1987], we had to limit our measurements to a region starting 20 km above the surface. The other boundary was chosen to be 90 km from the nucleus where the jets tend to merge with the background. Exception had to be made for the closest images where the smaller field of view limited the distance from the nucleus for which measurements could be made. Samples were taken at 0.5 or 1.0 km steps, depending on the image resolution.

3. Data analysis and results

The observed brightness at each point on an image is due to the combination of sunlight scattered by dust and by gas. Although within the spectral range of our filters no strong emission lines are present, the 5165 A line of C_2 can contribute. We have applied, with some modifications, the method of Larson and Sekanina [1984] to estimate the ratio of the dust to gas brightness contributions. These modifications were necessary because the images were taken from within the coma and because of the change in perspective caused by the proximity of the spacecraft relative to the ground observations. The changing velocities of the dust and gas components were also non negligible on some of the images. The details of this analysis have been published elsewhere [Toth et al. 1987]. The results obtained are compatible with the expectation, i.e. the brightness of the jets is due primarily to dust; the gas contribution is found to be negligible.

To analyze the brightness distribution along jets, the measured intensities were fitted to a function parametrized as $A(r-r_o)^p$; where r_o is the radius of the jet source on the nucleus. As previously mentioned, $r-r_o$ is the real, not projected distance. For a given feature identified on different images, the parameters r_o and p should, of course, be constant. The parameter A varies with varying phase angle and with the different color filters.

The computer code RFIT was used to fit the parameters; developed by Z. Szatmáry [1977] for application in reactor physics. The main advantage of this code is that it is able to identify break-points in the distributions.

As the number of useful data points axis are limited, we were unable to fit all of the parameters simultaneously, and we had to try different combinations.

The parameter r_o was chosen to be an average 5 km for all the data sets as geometrical considerations based on the jet source analysis [Smith et al. 1986] suggested. This value was also tested with many fitting procedures.

For each feature we then did a multi-sample fit: fitting a different A parameter for each sample (for each image) with a common exponent and checking the statistical confidence to determine the acceptability of the fit. To our surprize, the analyses found a break-point in the distribution for all of the data. This is shown in Table 2. We are forced to conclude, therefore, that in the brightness distribution does indeed undergo a change in slope close to the nucleus, and that it occurs in the range 30-40 km from the nucleus, for all the features analysed.

This result was further confirmed by the point-drop method which is also a part of RFIT. In this case an individual fit was performed for each data set in different radial ranges. As illustrative example is shown in Table 3. for the jet-core C. This analysis yielded the same break-point ranges.

As previously stated , the derived values of A - after proper normalization which takes into account the filter bandwith and exposure time - should be related to the optical scattering phase function of the dust. The normalized values of A are summarized in Table 4, and plotted in Fig. 1. The solid curve is the function derived by Divine [1981]. Our results and those of Divine are mutually consistent. The fairly large errors are due to the error in the determination of r_o. We then proceeded to determine whether grain disintegration might be a plausible explanation for our results.

4. A simple model for grain disintegration

Dust grains leaving the surface have an initial temperature of 200-300 K depending on whether they originate from pristine ice or they come from the surface regolith [Szegö, 1987]. After leaving the surface, the ejected dust grains undergo heat shock, since they are heated by solar radiation but cooled only by their own black body radiation. The solar flux at the encounter point (0.9 AU) is about 1700 W/m^2, which yields about 400 K for grains larger than the actual wavelength (those smaller reach a temperature of approximately 600-700 K). Since the dust heat capacity is about 1 Ws/g/K [Divine et al., 1986], the new temperature is reached almost instantaneously.

We suggest that due to this heat shock, sputtering quickly begins on the surface of the dust grains. If the grains disintegrate, the new surface areas are always greater than those of the original grains. For spheres, the surface gain is $(1-x)^q+x^q > 1$, where x is the fractional volume of one component of a fractured sphere and $q=2/3$. The maximal surface gain is about 25% and occurs when the sphere splits in half.

Let us assume that the gain in surface area after sputtering or disintegration is equal to $1+a$ on the average, where $a<1$. We further assume that the disintegration is proportional both to the actual volume and to the elapsed time. Since the particle velocity can be considered to be constant over the range of our investigation, elapsed time is proportional to distance. Thus, the disintegration probability at a certain distance is proportional to $(1-b)^r$, where $b<1$ describes the volume decrease and r denotes the

distance.

As the change of the observed brightness is proportional to the change of the scattering surface, the brightness change ratio at a given point is proportional to $(1+a)^{((1-b)^r)}$, and for the whole trajectory to

$$(1+a)^{(1-b)^r/\ln(1-b)} \quad . \qquad (1)$$

While we do not claim uniqueness for this model, we note that it is consistent with our observation and phisically can not be excluded. From (1) it is clear that for large r (e.g. r>40 km) this factor approaches unity; hence further out the brightness change is due only to the spread of the dust beam, i.e. it goes as 1/r. Closer to the nucleus, the brightness will change more slowly than 1/r. Values of about 0.1 for a and b derived from the data are not unrealistic.

This model also explains the unexpectedly large number of small dust particles which are born in the process of sputtering, and from this it follows that the terminal valocity of the grains have bigger spread than in earlier models.

5. Conclusion and discussion

The investigation of the radial brightness distribution of the near nucleus jets shows unambiguously that there is a breakpoint in all three of the jets that we studied as well as the region between the jets. In those cases investigated, this break occurs between 40 and 50 km from the nucleus. Farther than that the brightness distribution changes as 1/r. Closer than that, 1/r behaviour is found to be inconsistent with the data. However, there is no single radial exponent valid for a whole region; the exponent depends both on the individual jet and on the range selected. As there seems to be no difference between the behaviour of the three jets and the inter-jet region, we conclude that this region is also made up of unresolved jets.

The GIOTTO imaging team also reported deviations from the 1/r brightness distribution [Thomas and Keller, 1987]; however, no statistical analysis was presented with the observations, so its confidence level is not clear.

Several possible explanations can be devised for the observation presented. If the dust volume density sufficiently high, the jet is optically thick and some dust particles may screen others from the observer. As the dust expands, more particles begin to appear in the field of view,

resulting in brightness falloff that is less steep than 1/r. The observed optical thickness, however, contradicts this explanation [Sagdeev et al., 1985; Keller et al., 1987].

Another possibility is the conspiracy of a peculiar dust source distribution and non-uniform emission rate. This was investigated by [Huebner and Boice, 1987]. While it is true that certain model distributions cause deviations from the 1/r behaviour close to the surface, in our opinion the use of such circumstances would be very tedious and artificial to explain breakpoints in the distribution function for all the four features in the range that we have examined.

The most likely explanation, in our view, is dust grain disintegration. Theoretically, it was expected. Huebner et al. [1987] in identifying the first polimer in Comet Halley, noted that due to its volatility, the dust particles containing it will fragment. Wallis et al. [1987] have reported evidence for evaporations of organic grains. While not a unique model, grain disintegration is consistent both with theory and observation.

References

Abergel A. & Bertaux J.L.: Astron. & Astrophys., 187, 829, 1987.
Cosmovici C. B., et al.: Nature, 332, 705, 1988.
Divine N.: ESA SP-174, 47, 1981.
Divine N., et al.: Space Sci. Rev., 43, 1, 1986.
Gombosi T.I., et al.: Proc. of the International Conf. on Cometary Expl., Vol.II, 99, 1982.
Grün E., et al.: ESA SP-278, 305, 1987.
Huebner W.F., et al.: ESA SP-278, 163, 1987.
Huebner W.F. & Boice D.C.: 1987, In preparation
Justusson B.I.: Topics in Applied Physics, Vol. 43, Springer Verlag, Berlin, Heidelberg, New York, 1981.
Keller H.U., et al.: ESA SP-250 VOL. II., 359, 1986.
Kitamura Y.: Icarus, Vol. 66, 241, 1986.
Kitamura Y.: Icarus, 72, 555, 1987.
Larson S. & Sekanina Z.: Astron. J. Vol. 89, 571, 1984.
Sagdeev R.Z., et al.: Adv. Space Res.. Vol. 5, No.12, 95, 1985.
Sagdeev R.Z., et al.: Astrophys. Lett. Vol.25, No.4, 247, 1987.
Sagdeev R.Z. & Szegö K.: KFKI-1987-35/C, 1987, to appear in: Ellis Horwood Limited, Comet Halley 1986, London
Smith B.A., et al.: ESA SP-250, Vol. II, 227, 1987.
Szatmáry Z.: KFKI-1977-43, 1977.
Szegö K.: Astrophys. & Space Sci. Vol. 144, 439, 1988.
Thomas N. & Keller H.U.: ESA SP-278, 337, 1987.
Toth I., et al.: ESA SP-278, 343, 1987.
Wallis M.K., et al.: ESA SP-250, Vol.II, 251, 1986.

TABLE 1

Image number	Time[a]	Range	Resolution[b]	Field of view[b]	Phase angle[c]	Sun angle[c]	Filter[d]
1174	−370.5 s	29 540 km	1.03 km	265 km	98.4	89.0	NIR
1178	−282.9 s	23 140 km	0.81 km	207 km	94.0	89.3	VIS
1182	−197.0 s	17 120 km	0.60 km	153 km	86.6	89.6	RED
1186	−101.7 s	11 200 km	0.39 km	100 km	69.3	69.3	GLS
1190	− 1.5 s	8030 km	0.28 km	72 km	28.7	28.7	NIR
1194	+ 98.7 s	11 040 km	0.39 km	99 km	23.5	23.5	VIS
1198	+187.3 s	16 460 km	0.58 km	147 km	38.7	38.7	RED
1202	+280.5 s	22 970 km	0.80 km	206 km	46.6	46.8	GLS
1206	+372.7 s	29 700 km	1.04 km	266 km	51.3	51.3	NIR
1210	+467.9 s	36 790 km	1.29 km	330 km	54.3	54.3	VIS
1214	+558.1 s	43 570 km	1.53 km	390 km	56.2	56.2	RED

[a] Time is relative to closest approach, which occurred at 0720.0 UT

[b] The pixels in the Vega CCD detectors are rectangular, measuring 18 × 24 μm. This results in differing resolution in the vertical and horizontal directions and in a rectangular field of view. The values given here represent an average of the two orthogonal directions. Resolution is defined as a line pair.

Phase angle is the sun-comet-spacecraft angle. Sun angle is the direction of the sun in each frame, measured counter-clockwise from the top, which is also ecliptic north.

[d] GLS = clear glass, VIS = Visual, RED = Red, NIR = Near Infrared. See Sagdeev et al. (1987).

TABLE 2

POSITION OF THE BREAK POINT IN THE RADIAL BRIGHTNESS DISTRIBUTIONS FOR THREE JETS AND JET-FREE REGION FROM VEGA-2 IMAGES

IMAGE	DATA SAMPLES			
	A	B	C	D
1174	-	30 - 32	52	48 - 52
1178	33 - 35	26 - 27	35	49 - 54
1182	32 - 37	35	29 - 44	29
1186	27	26	26 - 35	30 - 35
1198	-	< 40	26 - 34	38
1202	-	-	-	~40
1206	-	-	<47	39 - 45
1210	-	-	-	<40
1214	-	-	-	<49

SAMPLES:

A JET BETA = -67 DEG.
B JET BETA = -54 DEG.
C JET BETA = -40 DEG.
D INTERMEDIATE REGION.

TABLE 3

PARAMETER FIT FOR A SINGLE SAMPLE OF JET
BETA = -40 DEG. THE FITTED FUNCTION IS
$B(R) = A(R-R_o)^P$ R = -5KM D(P) IS THE 1SD
ERROR OF P

IMAGE	RANGE [KM]	A	P	D(P)	SAMPLE [N1 - N2]
1174	20 - 90	1886.2	-0.6803	0.0108	1 - 71
	30 - 90	2766.0	-0.7729	0.0087	11 - 71
	40 - 90	3678.3	-0.8402	0.0065	21 - 71
	50 - 90	4088.8	-0.8645	0.0095	31 - 71
	60 - 90	5032.6	-0.9118	0.0137	41 - 71
	70 - 90	5949.6	-0.9494	0.0305	51 - 71
1178	20 - 90	2616.7	-0.7728	0.0134	1 - 71
	30 - 90	3854.5	-0.8669	0.0108	11 - 71
	40 - 90	5211.1	-0.9382	0.0125	21 - 71
	50 - 90	6913.3	-1.0036	0.0184	31 - 71
	60 - 90	8892.5	-1.0611	0.0340	41 - 71
1182	20 - 80	2270.4	-0.8697	0.0112	1 - 61
	30 - 80	3278.3	-0.9609	0.0104	11 - 61
	40 - 80	3120.6	-0.9491	0.0184	21 - 61
	50 - 80	4455.7	-1.0325	0.0295	31 - 61
	60 - 80	5247.7	-1.0716	0.0420	41 - 61
1186	15 - 50	1927.1	-0.6875	0.0094	1 - 71
	20 - 50	2426.8	-0.7500	0.0090	11 - 71
	25 - 50	2907.8	-0.8071	0.0093	21 - 71
	30 - 50	.2	-0.8525	0.0126	31 - 71
1190	8 - 30	851.3	-0.7934	0.0094	1 - 89
	10 - 30	978.6	-0.8366	0.0107	9 - 97
	12 - 30	1200.6	-0.8991	0.0086	17 - 89
	14 - 30	1292.0	-0.9214	0.0084	25 - 89
	16 - 30	1236.8	-0.9084	0.0105	33 - 89
	18 - 30	1292.7	-0.9215	0.0130	41 - 89
	20 - 30	1485.1	-0.9621	0.0162	49 - 89
1198	20 - 80	3781.7	-1.0933	0.0091	1 - 61
	30 - 80	4490.0	-1.1362	0.0150	11 - 61
	40 - 80	5594.7	-1.1890	0.0254	21 - 61
	50 - 80	7391.6	-1.2546	0.0484	31 - 61
1206	20 - 90	3401.0	-0.8342	0.0075	1 - 71
	30 - 90	4325.7	-0.8927	0.0083	11 - 71
	40 - 90	5454.0	-0.9474	0.0105	21 - 71
	50 - 90	7583.0	-1.0238	0.0103	31 - 71

TABLE 4

ANALYSIS OF THE NORMALIZED AMPLITUDE PARAMETER A (SEE TEXT)

IMAGE	DATA SAMPLES				PHASE ANGLE
	A	B	C	D	[DEG.]
1174	0.0017	-	0.0022	0.0034	98.4
1178	0.0052	0.0054	0.0042	0.0058	94.0
1182	0.0064	0.0059	0.0043	0.0061	86.6
1186	0.0039	0.0023	0.0018	0.0031	69.3
1190	0.0075	0.0102	0.0080	0.0077	28.7
1198	0.0140	0.0159	0.0144	0.0153	38.7
1202	-	-	-	0.0029	46.8
1206	-	-	0.0040	0.0052	51.3
1210	-	-	-	0.0050	54.3
1214	-	-	-	0.0023	56.2

SAMPLES:

A JET BETA = -67 DEG.
B JET BETA = -54 DEG.
C JET BETA = -40 DEG.
D INTERMEDIATE REGION.

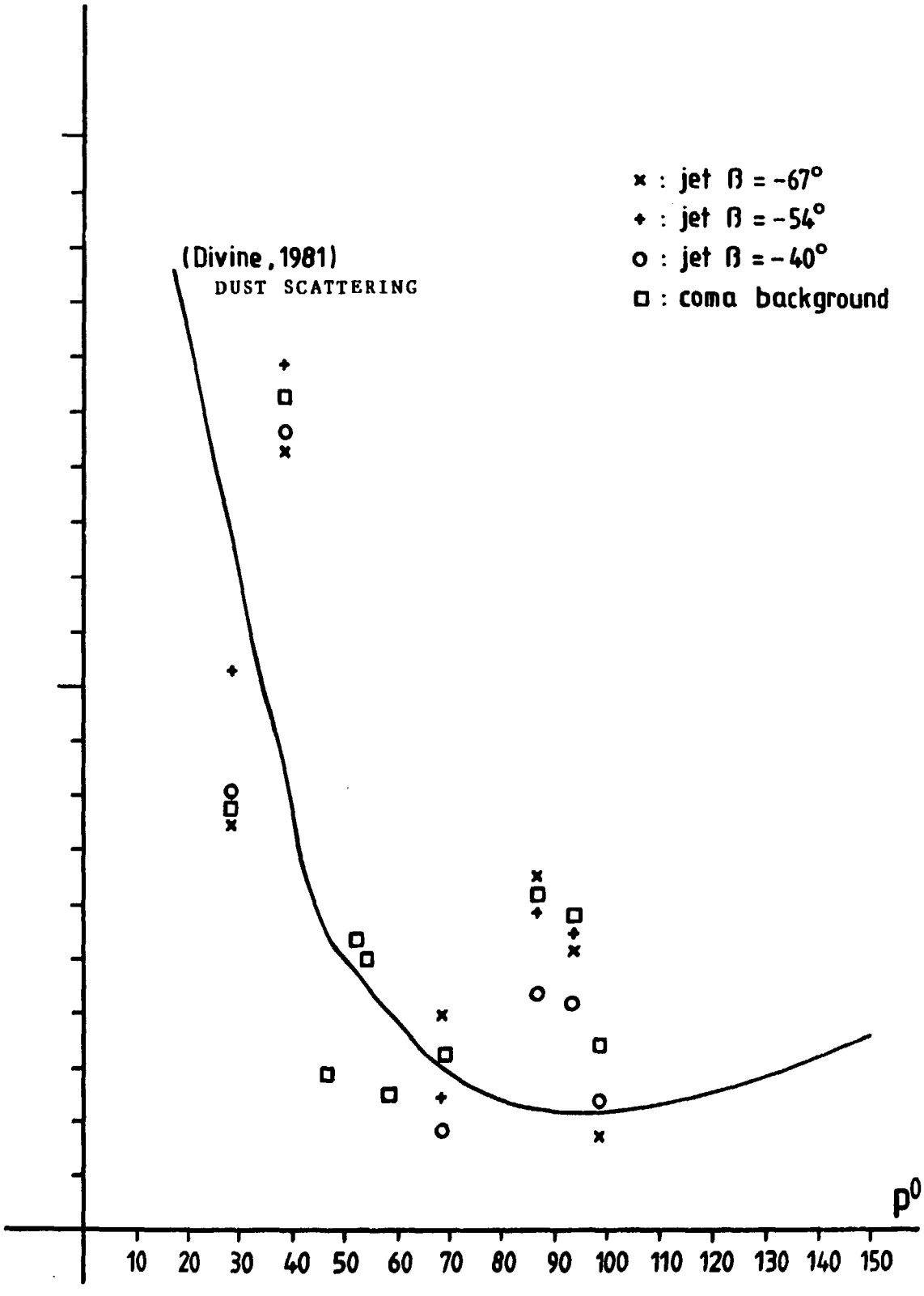
× : jet ß = -67°
✦ : jet ß = -54°
o : jet ß = -40°
□ : coma background
(Divine, 1981)
DUST SCATTERING
p⁰
10 20 30 40 50 60 70 80 90 100 110 120 130 140 150

FIG. 1.

The issues of the KFKI preprint/report series are classified as follows:

A. Particle and Nuclear Physics
B. General Relativity and Gravitation
C. Cosmic Rays and Space Research
D. Fusion and Plasma Physics
E. Solid State Physics
F. Semiconductor and Bubble Memory Physics and Technology
G. Nuclear Reactor Physics and Technology
H. Laboratory, Biomedical and Nuclear Reactor Electronics
I. Mechanical, Precision Mechanical and Nuclear Engineering
J. Analytical and Physical Chemistry
K. Health Physics
L. Vibration Analysis, CAD, CAM
M. Hardware and Software Development, Computer Applications, Programming
N. Computer Design, CAMAC, Computer Controlled Measurements

The complete series or issues discussing one or more of the subjects can be ordered; institutions are kindly requested to contact the KFKI Library, individuals the authors.

Title and classification of the issues published this year:

KFKI-1988-01/A L. Diósi	On the motion of solids in modified quantum mechanics
KFKI-1988-02/D Bakos J.	Thermonuclear plasmaphysical research in the Central Research Institute for Physics (1986-1987) (in Hungarian)
KFKI-1988-03/E A. Jákli et al.	A special shear method of alignment for smectic liquid crystals
KFKI-1988-04/A L. Diósi et al.	Restoration of 2-π^0 inclusive distribution from observed 2-γ data
KFKI-1988-05/A L. Diósi	Continuous quantum measurement and Itô formalism
KFKI-1988-06/E G. Konczos et al.	Amorphous alloys bibliography 1984-1987: papers from the Central Research Institute for Physics /Budapest/ and cooperating institutions
KFKI-1988-07/E L. Cránásy et al.	Superconductivity without rear earth metals in pure and Fe dopped Bi-Cu-Sr-Ca oxide systems (in Hungarian)
KFKI-1988-08/B B. Lukács et al.	Galaxy formation from tepid inflation
KFKI-1988-09/E I. Furó et al.	Fluctuating electronic magnetic moment in $YBa_2Cu_3O_{6.2}$: an NMR and NQR study
KFKI-1988-10/M A.K. Sdaa et al.	The analysis of the alternating bit protocols
KFKI-1988-11/M R. Wittmann	Introduction to Milner's Calculus of Communicating Systems
KFKI-1988-12/E A. Rockenbauer et al.	Magnetic field dependent microwave absorption in the multiphase Bi-Sr-Ca-Cu oxide system

KFKI-1988-13/M M. Barbuceanu et al.	XRL: A layered knowledge processing architecture able to enhance itself
KFKI-1988-14/B L. Diósi et al.	Mapping the van der Waals state space
KFKI-1988-15/E L. Mihály et al.	Experimental studies on high temperature superconductors
KFKI-1988-16/M P. Ecsedi-Tóth et al.	The LOTOS specification language /in Hungarian/
KFKI-1988-17/A A. Frenkel	The reduction of the Schrödinger wave function and the emergence of classical behavior
KFKI-1988-18/E N. Kroó et al.	Decay time measurement of surface plasmons on silver gratings
KFKI-1988-19/A P. Hidas	The inclusive production of the Ξ^- particles in 280 GeV/c muon-proton interactions
KFKI-1988-20/A T. Dolinszky et al.	A new class of analytically solvable quantum scattering problems
KFKI-1988-21/A L. Diósi	Localized solution of simple nonlinear quantum Langevin-equation
KFKI-1988-22/E H. Kuzmany et al.	Oxygen induced phase changes in $YBa_2Cu_3O_{6+\delta}$. Transport, structural and spectoscopic evidence
KFKI-1988-23/E K. Tompa et al.	^{205}Tl NMR spin echo investigations in multiphase Tl-Ba-Ca-Cu oxide superconductors
KFKI-1988-24/G R. Kozma et al.	Experimental study of the field-of-view of neutron detectors towards thermohydraulic perturbances
KFKI-1988-25/K K. Fodor-Csorba et al.	Structure-activity relationship studies on the antidotes of thiocarbamate herbicides /in Russian/
KFKI-1988-26/D D.N. Yundev et al.	Measurement of the absorption coefficient and index of refraction of templene in the submillimetre wave range
KFKI-1988-27/E B. Sas et al.	Thermoelectric power and anisotropic magneto-resistance of Fe-TM-B-amorphous alloys
KFKI-1988-28/M S. Wagner-Dibuz	Protocol consultant, an expert system for protocol engineering
KFKI-1988-29/E L. Rosta	Neutron physical properties of a multidisc velocity selector
KFKI-1988-30/A B. Kämpfer et al.	Anisotropic nuclear matter with momentum-dependent interaction
KFKI-1988-31/E L. Bottyán et al.	Evidence for Fe^{4+} in $YBa_2(Cu_{1-x}M_x)_3O_{7-y}$ (M=^{57}Co, ^{57}Fe) by absorption and emission Mössbauer spectroscopy
KFKI-1988-32/C K. Szegő et al.	Surface and dust features seen on the nucleus of Comet Halley
KFKI-1988-33/C K. Szegő et al.	Dust photometry in the near nucleus region of Comet Halley

Kiadja a Központi Fizikai Kutató Intézet
Felelős kiadó: Szegő Károly
Szakmai lektor: Varga András
Nyelvi lektor: Somogyi Antal
Példányszám: 284 Törzsszám: 88-424
Készült a KFKI sokszorosító üzemében
Felelős vezető: Töreki Béláné
Budapest, 1988. augusztus hó